Molecular Modelling of Family GH16 Glycoside Hydrolases: Potential Roles for Xyloglucan Endotransglucosylases/Hydrolases in Cell Wall Modification in the Poaceae

Marco Strohmeier[1], Maria Hrmova[2], Markus Fischer[1], Andrew J. Harvey[2], Jürgen Pleiss[1] and Geoffrey B. Fincher[2,*]

[1]Institute of Technical Biochemistry at the University of Stuttgart, Allmandring 31, D-70569 Stuttgart, Germany and the [2]Faculty of Sciences, School of Agriculture and Wine, and the Australian Centre for Plant Functional Genomics, The University of Adelaide, Waite Campus, Glen Osmond, South Australia 5064, Australia.

*For correspondence (fax +61 8 8303 7109; email geoff.fincher@adelaide.edu.au)

Running title: Homology modelling of family GH16 glycoside hydrolases

Keywords: database, β-galactanases, (1,3/1,3;1,4)-β-D-glucan endohydrolases, (1,3;1,4)-β-D-glucan endohydrolases, homology modelling, xyloglucan endotransglucosylases.

Word count: total, approximately 8,500; summary 200.

Abbreviations: EST, expressed sequence tag; LED, Lipase Engineering Database; XTH, xyloglucan endotransglucosylase/hydrolase; 3D, three-dimensional.

Summary

Family GH16 glycoside hydrolases can be assigned to five sub-groups according to their substrate specificities, including xyloglucan endotransglucosylases/hydrolases (XTHs), (1,3)-β-galactanases, (1,4)-β-galactanases/κ-carrageenases, "non-specific" (1,3/1,3;1,4)-β-D-glucan endohydrolases and (1,3;1,4)-β-D-glucan endohydrolases. A structured family GH16 glycoside hydrolase database has been constructed (http://www.ghdb.uni-stuttgart.de) and provides multiple sequence alignments with functionally annotated amino acid residues and phylogenetic trees. The database has been used for homology modelling of seven family GH16 glycoside hydrolases, based on structural coordinates for (1,3;1,4)-β-D-glucan endohydrolases and a κ-carrageenase. In combination with multiple sequence alignments, the models predict the three-dimensional dispositions of amino acid residues in the substrate-binding and catalytic sites of XTHs and (1,3/1,3;1,4)-β-D-glucan endohydrolases, for which no structural information is available. Furthermore, they reveal similarities with the active sites of family GH11 (1,4)-β-D-xylan endohydrolases. From a biological viewpoint, the classification and molecular modelling establish structural and evolutionary connections between XTHs, (1,3;1,4)-β-D-glucan endohydrolases and xylan endohydrolases, and raise the possibility that XTHs from higher plants could be active not only on cell wall xyloglucans, but also on (1,3;1,4)-β-D-glucans and arabinoxylans, which are major components of walls in grasses. A role for XTHs in (1,3;1,4)-β-D-glucan and arabinoxylan modification would be consistent with the apparent over-representation of XTH sequences in cereal EST databases.

Introduction

Progressive changes in the composition of cell walls and in the fine structure of constituent polysaccharides are of central importance in plant development. Different cell types within a plant can be distinguished from each other by the chemistry and organization of their walls, and walls differ in a way that is related to developmental stage or to their exposure to different environmental conditions (Fincher, 1993; Pennel, 1998; Cosgrove, 1999; Carpita *et al.*, 2001). Wall composition and fine structure can also change in response to microbial attack, when rapid deposition of the polysaccharide callose and layers of lignin, together with the formation of a cross-linked protein network, create a physical barrier that is believed to impede the progress of invading fungal and bacterial pathogens (Mengden *et al*., 1996; Knogge, 2002). Thus, the wall is a dynamic structure in which newly-deposited polysaccharides can be modified or re-structured during normal growth and development, or in response to abiotic and biotic stresses.

Primary walls of dicotyledonous plants consist of a cellulosic network embedded in a matrix of complex polysaccharides of which xyloglucans, glucuronoarabinoxylans and pectic polysaccharides are most abundant (Carpita and Gibeaut, 1993). Extensive intermolecular hydrogen bonding between matrix phase polysaccharides and cellulose are thought to be important determinants of overall wall integrity (Fry, 1989; Hayashi, 1989; Carpita *et al.*, 2001). Walls of the monocotyledons are constructed in essentially the same way, although glucuronoarabinoxylans and (1,3;1,4)-β-D-glucans predominate in the matrix phase, particularly in the grasses; levels of pectic polysaccharides and xyloglucans are relatively low in these species (Carpita and Gibeaut, 1993). For example, xyloglucan levels in walls from barley (*Hordeum vulgare*) aleurone, starchy endosperm and young leaves are extremely low or absent (Sakurai and Masuda, 1978; Fincher, 1993). The highest xyloglucan content so far detected in barley cell walls is 8-10% in coleoptiles (D.M. Gibeaut, M. Pauly and G.B. Fincher, unpublished data). Xyloglucan levels in suspension-

cultured maize cells are about 4% (Rose *et al.*, 2002) and low levels are found in walls from the starchy endosperm of rice (Shibuya and Misaki, 1978; Shibuya *et al.,* 1983).

Xyloglucans are subject to modification following their initial deposition into the wall. In particular, their molecular mass distribution can be altered to simultaneously generate larger and smaller polysaccharide chains (Smith and Fry, 1991; Nishitani, 1997). This 'disproportionation' is catalysed by xyloglucan endotransglycosylases (EC 2.4.1.207) that are abundant in the apoplastic space during wall development. It is now known that xyloglucan-modifying enzymes include both xyloglucan endotransglycosylases (XETs) and xyloglucan endohydrolases (XEHs), which are collectively referred to as xyloglucan endotransglycosylases/hydrolases (XTHs) (Farkas *et al.*, 1992; Fanutti *et al.*, 1993; Rose *et al.*, 2002).

Our interest in barley XTHs was originally stimulated by observations that *XTH* sequences were surprisingly abundant in barley EST databases. These observations were consistent with earlier reports that XET activity extractable from vegetative tissues of grasses was higher than that extractable from dicotyledons (Fry *et al.*, 1992; Wu *et al.*, 1994). Given the low levels of xyloglucans in walls of most barley tissues, it seemed possible that the enzymes might be active on the more abundant matrix phase polysaccharides, namely the arabinoxylans and/or the (1,3;1,4)-β-D-glucans. In support of this possibility, it was recently reported that the molecular mass of xylans in walls of suspension-cultured maize cells increased dramatically in the first few hours after deposition in the walls (Kerr and Fry, 2003); this was suggestive of (1,4)-β-D-xylan transglycosylation activity.

Here, homology modelling has been used to develop potential three-dimensional (3D) structures for XTHs. The models have subsequently been compared with known 3D structures of enzymes that hydrolyse arabinoxylans and (1,3;1,4)-β-D-glucans, to assess the possibility that XTHs from grasses

could bind to and disproportionate these abundant wall constituents. The plant XTHs are all classified in the family GH16 group of glycoside hydrolases, although a small number of microbial XTHs are classified within family GH12 (Coutinho and Henrissat, 1999; http://afmb.cnrs-mrs.fr/CAZY/). Initial analyses of the family GH16 enzymes have revealed an evolutionary and structural link between higher plant XTHs and microbial (1,3;1,4)-β-D-glucan endohydrolases, while more detailed comparisons of active site regions have uncovered similarities between the XTHs and family GH11 (1,4)-β-D-xylan endohydrolases.

Results

EST database analysis reveals an abundance of XTH *sequences*

Analysis of cell wall-modifying enzymes and proteins from 345,000 barley ESTs from the NCBi web site revealed an abundance of *XTH* sequences in the databases. Although xyloglucans account for less than 5-10% of walls in most barley tissues, the *XTH* ESTs represent more than 20% of all ESTs encoding enzymes and proteins that have been implicated in the synthesis, re-structuring and/or degradation of major wall polysaccharides in barley (Figure 1a). Within the *XTH* ESTs, five genes account for most of the entries (Figure 1b). These highly represented genes are designated *HvXTH1* to *HvXTH5* (Figure 1b). Further analyses of the *XTH* sequences identified in Figure 1 showed that the barley genome carries at least 22 independent *XTH* genes (data not shown). The detection of additional *XTH* ESTs that did not overlap with regions used to define the 22 different genes would suggest that further *XTH* genes are likely to be present on the barley genome. Examination of the draft rice genome sequence (Goff, 2002) indicated that the rice genome carries at least 29 *XTH* genes (data not shown). Cellulose synthases (*CesA*s) comprise almost 25% of the barley ESTs while expansins, which are involved in wall elongation (Cosgrove, 1999), comprise about 15% of wall-modifying proteins in the barley EST databases (Figure 1a).

The family GH16 glycosyl hydrolases can be divided into five subgroups

The Lipase Engineering Database (LED) system (Fischer and Pleiss, 2003) was used to collect about 250 proteins from the family GH16 group of glycoside hydrolases, as in the CAZy Database (Coutinho and Henrissat, 1999). Based on multiple sequence alignment, phylogenetic analysis and substrate specificity the proteins were assigned to five subgroups, each of which has distinct substrate specificity. The subgroups included XTHs (102 proteins), (1,3;1,4)-β-D-glucanases (48

proteins), (1,3)-β-galactanases (10 proteins), (1,4)-β-galactanases/κ-carrageenases (5 proteins) and non-specific (1,3/1,3;1,4)-β-D-glucanases (60 proteins). The non-specific (1,3/1,3;1,4)-β-D-glucanases are able to hydrolyse either a (1,3)-β- or a (1,4)-β-D-glucosyl linkage in a β-D-glucan, provided there is an adjacent (1,3)-β-D-glucosyl linkage on the non-reducing terminal side of the linkage hydrolysed, and hence can hydrolyse either (1,3)-β-D-glucans or (1,3;1,4)-β-D-glucans (Høj and Fincher, 1995). The sequences of two SKN1 proteins, two KRE6 proteins and four putative β-D-glucan synthesis-associated proteins were assigned to the non-specific (1,3/1,3;1,4)-β-D-glucanase subgroup, as proposed previously (Barbeyron *et al.*, 1998). Several proteins classified in the CAZy Database as family 16 glycoside hydrolases (Coutinho and Henrissat, 1999), including four (1,3)-β-D-glucan recognition proteins, four gram-negative bacteria binding proteins, a p50 protein, an allergen, an external agarase and eight (1,3)-β-D-glucan-binding proteins, could not be assigned to any of the subgroups.

An unrooted phylogenetic tree showing a random selection of 56 enzymes of the 250 proteins from the five subgroups is shown in Figure 2. Inclusion of all 250 proteins resulted in a cluttered tree in which individual proteins were difficult to discern (Harvey *et al*., 2000). Enzymes for which 3D structures are available are indicated, together with enzymes used for subsequent modelling experiments (Figure 2). It appears that the large non-specific (1,3/1,3;1,4)-β-D-glucanase subgroup is centrally placed in the tree, and that the two smaller subgroups of β-galactanases and the two subgroups of (1,3;1,4)-β-D-glucanases and XTHs lie at the edges of the tree (Figure 2). Whether this means that the non-specific (1,3/1,3;1,4)-β-D-glucanase subgroup has acted as a common ancestor for the other four subgroups in family GH16 remains to be demonstrated.

Multiple sequence alignments further revealed that the catalytic nucleophile and the catalytic acid/base residues of the β-galactanases and non-specific (1,3/1,3;1,4)-β-D-glucanase subgroups were separated by four amino acid residues (Figure 3a), while those in the XTH and (1,3;1,4)-β-D-

glucanase subgroups were separated by three amino acid residues (Figure 3b). In the expectation that the different spacing of catalytic amino acid residues was likely to have an effect on substrate specificity and probably reflected an important evolutionary change in active site geometry (Michel *et al*., 2001), we have sub-divided the family GH16 enzymes into sub-family GH16a, comprising the β-galactanase and non-specific (1,3/1,3;1,4)-β-D-glucanase subgroups, where the catalytic residues are separated by four amino acid residues, and into sub-family GH16b, comprising the XTHs and the (1,3;1,4)-β-D-glucanases, where the catalytic residues are separated by three amino acid residues (Figure 3b).

The family GH16 database

The family GH16 glycoside hydrolase database (GHDB) is available on http://www.ghdb.uni-stuttgart.de. In addition to the alphabetic listing of family GH16 glycoside hydrolases, the database provides experimentally determined 3D protein structures, phylogenetic trees and multiple sequence alignments of the two sub-families GH16a and GH16b, and of each homologous subgroup therein. Functionally relevant residues such as the catalytic amino acid residues, aromatic substrate-binding residues, polar substrate-binding residues, Ca^{2+}-binding residues, cysteine residues involved in disulfide bridge formation, signal peptide sequences, potential *N*-glycosylation sites and residues involved in substrate processing are annotated according to the structural analyses described below, literature citations, and additional data extracted from GenBank and Protein Data Bank (Berman *et al.*, 2000). An automatic BLAST search is incorporated into the database for comprehensive analysis of the stored data.

Homology modelling of 3D structures from family GH16a

To compare the active site structures of family GH16 glycoside hydrolases, we performed homology modelling of selected members of the different subgroups, including XTHs and the non-specific (1,3/1,3;1,4)-β-D-glucanases, for which there are no experimentally determined 3D structures available. The 3D structure of a family GH16 (1,4)-β-galactanase/κ-carrageenase, from *Pseudoalteromonas carragenovora* (Michel *et al*., 2001) was used to predict the structure of the active site region of a second κ-carrageenase (272 amino acid residues out of 513) from *Zobellia galacinovorans* (Barbeyron *et al.*, 1998). The sequence identity between the target and template sequences was 39%, and the models suggested that secondary structural elements of the β-jelly roll fold of the enzymes were conserved, while differences were detected in loop regions (data not shown).

There are no crystal structures available for the non-specific (1,3/1,3;1,4)-β-D-glucanase group of family GH16 enzymes, but the solved structure of the *Pseudoalteromonas carragenovora* κ-carrageenase (Michel *et al.*, 2001) was used successfully as a template for molecular modelling of the non-specific (1,3/1,3;1,4)-β-D-glucanases from *Bacillus circulans* (Yahata *et al.*, 1990) and *Strongylocentrotus purpuratus* (Bachman and McClay, 1996). The sequences of the two non-specific (1,3/1,3;1,4)-β-D-glucanases contained 682 and 499 amino acid residues, respectively, and were about twice as long as the sequence of the available κ-carrageenase template structure. Differences in sequence lengths and domain compositions also made it difficult to align the non-specific (1,3/1,3;1,4)-β-D-glucanases with each other and with the κ-carrageenase template. However, the PRODOM program (Corpet *et al*., 1998) used in conjunction with multiple sequence alignment eventually allowed 268 out of 682 amino acid residues of the *Bacillus circulans* non-specific (1,3/1,3;1,4)-β-D-glucanase and 276 out of 499 amino acid residues of the *Strongylocentrotus purpuratus* non-specific (1,3/1,3;1,4)-β-D-glucanase to be aligned with the κ-carrageenase template sequence for homology modelling of the target protein structures (Figures 4a

and 4b). Both models again showed the typical family GH16 β-jelly roll fold and the 3D dispositions of the catalytically active region were conserved in both molecular models.

The substrate-binding clefts of both enzymes stretch across the surface of the protein, and in the case of the *Strongylocentrotus purpuratus* non-specific (1,3/1,3;1,4)-β-D-glucanase model, the cleft appears to be closed at the top (Figure 4b cf. 4a). Nevertheless, the dispositions of the catalytic amino acid residues and of the aromatic residues that are believed to be involved in substrate binding are similar. In addition, the active site aromatic residue that distinguishes the various subgroups [Trp118 in the κ-carrageenase from *Pseudoalteromonas carragenovora*, a Phe residue in the (1,3;1,4)-β-D-glucanases, and a Tyr residue in the XTHs; Figure 3a) is located in a similar position in all enzymes (Figures 4a and 4b). The conservation of these residues in cartesian space around the catalytic site (Figure 4) is consistent with their conservation in the amino acid sequence alignments of the enzymes (Figure 3a).

The protein sequence identities, RMS deviations, overall G-factors and Ramachandran plot statistics for template and target sequences of selected members from family GH16a are shown in Table 1. Despite the relatively low sequence identity values, the figures indicate that the models constructed for the non-specific (1,3/1,3;1,4)-β-D-glucanase from the κ-carrageenase template sequence are acceptable.

Homology modelling of 3D structures from family GH16b

In sub-family GH16b the 3D structures of two *Bacillus* (1,3;1.4)-β-D-glucanases have been solved by X-ray crystallography (Hahn *et al*., 1995). Based on sequence identities of nearly 60% between template and target sequences, it was possible to use the solved 3D structures to model the structure of a (1,3;1.4)-β-D-glucanase from *Bacillus brevis* (Louw *et al.*, 1993) and 219 of 330 amino acid

residues of a (1,3;1,4)-β-D-glucanase from *Clostridium thermocellum* (Schimming *et al.*, 1992). The only differences between the two solved structures and the two models were in loop regions of the enzymes; all secondary structural elements, residues required for substrate binding, and the 3D dispositions of catalytic residues were conserved (data not shown).

Amino acid sequence identities of about 30% allowed the 3D structures of the two *Bacillus* (1,3;1.4)-β-D-glucanases to be used as templates to build reliable models of three XTHs, namely the XTHs from *Vigna angularis* (175 of 292 amino acid residues) (Okazawa *et al.*, 1993), and *Vitis labrusca* (197 of 291 amino acid residues) (Ishimaru and Kobyashi, 2002). Because the template sequences of the *Bacillus* (1,3;1.4)-β-D-glucanases lacked about 100 amino acid residues found at the COOH-termini of the XTH target sequences, these regions of the XTH proteins could not be modelled. However, the catalytic amino acid residues of the two modelled XTHs were conserved and similar in spatial disposition to catalytic residues of the (1,3;1.4)-β-D-glucanases, as were substrate-binding aromatic residues and the distinguishing aromatic residues Phe92 from the (1,3;1.4)-β-D-glucanases and Tyr75 from the XTHs (Figures 4c and 4d). Again, the conservation of these residues in cartesian space around the catalytic site is consistent with their conservation in the amino acid sequences of the enzymes (Figure 3b) and reliability checks showed acceptable values for the models (Table 1). In contrast, models of the XTHs calculated using the structure of the *Pseudomonas carragenovora* κ-carrageenase as template showed distorted active site structures (data not shown), which showed that this template was not suitable for modelling XTHs.

The substrate-binding cleft in the XTH models appears to be somewhat wider than that in the (1,3;1.4)-β-D-glucanase templates (Figures 4c and 4d). Multiple sequence alignments of template and target sequences, together with alignments of all sequences belonging to the XTH subgroup showed a set of conserved amino acid residues that are located in the substrate binding cleft of the XTHs. The frequencies of these residues are shown in Table 2. Amino acid residues corresponding

to Tyr95, His103, Phe126, Tyr190 and Trp194 in the XTH of *Vigna angularis* are conserved in the substrate-binding cleft of the two modelled XTH structures (Figure 4d and Table 2). The highly conserved His83 and Asp87 residues of the XTHs correspond to Trp103 and Asp107 of the *Bacillus macerans* (1,3;1,4)-β-D-glucanase, respectively. These residues are likely to stabilize the catalytic nucleophile through hydrogen bonds (Keitel *et al*., 1993) and Asp87 may take part in proton trafficking (Michel *et al.,* 2001). Similarly, Tyr75 of the *Vigna angularis* XTH corresponds to Phe92 of the *Bacillus macerans* (1,3;1,4)-β-D-glucanase (Table 2), and is 5-7 Å from the Oε1 and Oε2 of the catalytic amino acid residues, while Tyr170 of the *Vigna angularis* XTH and corresponding amino acid residues in other XTHs are in the same position as Met180 of the *Bacillus macerans* (1,3-1,4)-β-D-glucanase (Table 2). Thus, these Met and Tyr residues are conserved in both the (1,3;1,4)-β-D-glucanase and XTH subgroups of family GH16b enzymes (Figure 3 and Table 2). Amino acid residues Asn121 and Glu131 of the *Bacillus macerans* (1,3-1,4)-β-D-glucanase also involved in substrate binding (Hahn *et al*., 1995) and are conserved in the XTHs; they correspond to Asn104 and Glu114 of the *Vigna angularis* XTH. The two aromatic amino acid residues in positions corresponding to Tyr24 and Tyr94 of the *Bacillus macerans* (1,3-1,4)-β-D-glucanase could not be detected in the sequences and the modelled 3D structure of the XTHs (Figures 3, 4c and 4d).

Another difference between the XTHs and the (1,3;1,4)-β-D-glucanases of the family GH16b subgroup is the insertion in the XTHs of three amino acid residues ProTyrXxx, where Xxx is a non-conserved amino acid residue, at a position corresponding to $Pro_{98}Tyr_{99}Ile_{100}$ in the *Vigna angularis* XTH structure (Table 2; Figure 3). The insertion is located in the modelled structure at the beginning of the central β-sheet, close to the Glu89 at substrate-binding subsite +2 or -2, so that the Tyr residue points towards the catalytic amino acid residues and the bound substrate.

XTH models share similarities with (1,4)-β-D-xylan endohydrolase 3D structures

When the model of the family GH16 *Vigna angularis* XTH is compared with the 3D structure of the family GH11 (1,4)-β-D-xylan endohydrolase from *Aspergillus niger* (Krengel and Dijkstra, 1996), significant differences in the shapes of the substrate-binding clefts are evident (Figure 5). The XTH cleft is relatively broad, which might be related to the greater width of the (1,4)-β-D-glucan backbone of the XTH substrate compared with the (1,4)-β-D-xylan substrate of the (1,4)-β-D-xylanase, and the top of the (1,4)-β-D-xylanase cleft appears to be closed. As expected for glycosyl endohydrolases, hydrophobic residues are located along the substrate-binding clefts of both types of enzyme (Figure 5). Nevertheless, both families GH11 and GH16 exhibit β-jelly roll folds (Coutinho and Henrissat, 1999) and when the 3D arrangements of catalytic amino acid residues and other residues close to the catalytic sites are compared between the family GH16 *Bacillus macerans* (1,3;1,4)-β-D-glucanase, the family GH16 *Vigna angularis* XET model, and the family GH11 *Aspergillus niger* β-D-xylan endohydrolase, clear similarities are observed. In Figure 6, the catalytic acid/base and catalytic nucleophile residues of the three enzymes are presented in a similar orientation. Approximately parallel β-strands in the region of the catalytic site carry aromatic residues that have similar 3D dispositions in relation to the catalytic residues. The Asp87 residue located between the catalytic residues in the (1,3;1,4)-β-D-glucanases and XTHs (Figures 6a and 6b) is not seen in the endoxylanase, where Tyr 81 is placed in a similar position (Figure 6c).

For a more detailed comparison, the catalytic residues and the Asp/Tyr residues that are located between these in the XTH models and the β-D-xylan endohydrolase structure were superposed. This shows that an "aromatic triad" of three aromatic amino acid residues that are important for substrate binding in the *Aspergillus niger* β-D-xylan endohydrolase, namely Tyr10, Tyr164 and Trp172 (Tahir *et al.*, 2002) has the same relative position in 3D space as a triad of three aromatic amino acid residues, namely Trp174, Tyr170 and Tyr99, in the *Vigna angilaris* XTH (Figures 6b cf. 6c). Aromatic amino acid residues corresponding to Tyr6 and Tyr89 of the *Aspergillus niger* β-D-

xylan endohydrolase, also identified as important for catalytic activity (Tahir *et al.,* 2002), could not be identified unequivocally through the comparison of the 3D structures. Furthermore, the aromatic platform of Tyr75 in the *Vigna angilaris* XTH overlaps with that of Tyr70 in the *Aspergillus niger* β-D-xylan endohydrolase (Figures 6b and 6c; Table 2). All other subgroups of the family GH16 glycoside hydrolases, namely the (1,3;1,4)-β-D-glucanases, (1,3)-β-galactanases, (1,4)-β-galactanases/κ-carrageenases and "non-specific" (1,3/1,3;1,4)-β-D-glucanases do not show this "aromatic triad" pattern in the active site (Figures 3, 4 and 6a).

Discussion

Over 20% of entries that encode cell wall-modifying enzymes or proteins in the large barley EST databases correspond to mRNAs for the XTH group of higher plant enzymes (Figure 1). Given that barley cell walls usually contain very low amounts of the XTH substrate xyloglucan, which is of relatively low abundance in the Poaceae more generally, this high level of XTH ESTs is surprising. One of several possible explanations for the higher than expected number of XTH entries is that the substrate specificity of the enzymes is broader than originally believed and that they catalyse the hydrolysis or transglycosylation of other polysaccharides that are more abundant than xyloglucans in barley cell walls. The most abundant non-cellulosic polysaccharides of barley walls are arabinoxylans and (1,3;1,4)-β-D-glucans (Fincher, 1993; Carpita *et al*., 2001). We therefore modelled XTH enzymes against the known 3D structures of related family GH16 (1,3;1,4)-β-D-glucan hydrolases and compared the active site regions with those of family GH11 (1,4)-β-D-xylan endohydrolases, in an attempt to identify any structural and hence evolutionary linkages between enzymes that bind xyloglucans, arabinoxylans and (1,3;1,4)-β-D-glucans.

The higher plant XTHs have been classified by Coutinho and Henrissat (1999) into the family GH16 group of glycosyl hydrolases. This family can be divided into five subgroups on the basis of differences in their substrate specificities (Figure 2). Firstly, a subgroup of (1,3)-β-galactan endohydrolases (EC 3.2.1.81) can hydrolyse (1,3)-β-galactosyl linkages in complex polysaccharides that include agarose (Michel *et al*., 2001). The second subgroup of enzymes (EC 3.2.1.83) are specific for (1,4)-β-galactosyl linkages in other complex polysaccharides that contain sulphated and anhydro-galactosyl residues, including κ-carrageenan and keratin sulphate (Kloareg and Quatrano 1988). The third subgroup includes the "non-specific" (1,3/1,3;1,4)-β-D-glucan endohydrolases (EC 3.2.1.6). These are non-specific insofar as they can hydrolyse both (1,3)- and (1,4)-linkages in β-D-glucans, provided there is an adjacent (1,3)-β-D-glucosyl residue on the non-reducing terminal

side of the linkage hydrolysed (Anderson and Stone, 1975; Høj and Fincher, 1995). These enzymes can therefore hydrolyse both (1,3)-β-D-glucans and (1,3;1,4)-β-D-glucans. The fourth subgroup comprises (1,3;1,4)-β-D-glucan endohydrolases (EC 3.2.1.73). These are absolutely specific for the hydrolysis of a (1,4)-β-D-glucosyl linkage, but only if there is an adjacent (1,3)-β-D-glucosyl residue towards the non-reducing end of the substrate. These enzymes can therefore hydrolyse only (1,3;1,4)-β-D-glucans (Parrish *et al*., 1960; Høj and Fincher, 1995; Hrmova and Fincher, 2001). The fifth subgroup contains xyloglucan-modifying enzymes that are collectively referred to as xyloglucan endotransglycosylases/hydrolases (XTHs; EC 2.4.1.207), but include both xyloglucan endotransglycosylases (XETs) and xyloglucan endohydrolases (XEHs) (Farkas *et al.*, 1992; Fanutti *et al.*, 1993; Rose *et al.*, 2002). These enzymes hydrolyse (1,4)-β-D-glucosyl linkages specifically in xyloglucans, but those with XET activity can also catalyse transglucosylation reactions, in which the non-reducing terminal product of the hydrolysis reaction can subsequently be transferred onto another xyloglucan molecule (Rose *et al.*, 2002).

Although members of the XTH subgroup are found exclusively in higher plants, while members of the other four subgroups are of microbial origin (Coutinho and Henrissat, 1999), the classification of XTHs with microbial (1,3;1,4)-β-D-glucan endohydrolases in family GH16 establishes an evolutionary link between the two enzyme groups. It is noteworthy that higher plants of the Poaceae also synthesise (1,3;1,4)-β-D-glucan endohydrolases, but these have a completely different protein fold, they are classified in family GH17, and clearly converged with the microbial (1,3;1,4)-β-D-glucan endohydrolases along a distinct evolutionary route (Høj and Fincher, 1995; Coutinho and Henrissat, 1999). The plant XTHs and microbial (1,3;1,4)-β-D-glucan endohydrolases of sub-family GH16b show a number of features that distinguish them from the other three subgroups of the family. In particular, their catalytic amino acid residues are separated by three amino acid residues, in contrast to members of the other three subgroups that comprise sub-family GH16a, in which four amino acid residues separate the catalytic amino acid residues (Figure 3). Moreover, the

plant XTHs and microbial (1,3;1,4)-β-D-glucan endohydrolases of sub-family GH16b have a distinguishing Phe or Tyr residue in the vicinity of the catalytic amino acid residues, in a position that is occupied by a Trp in sub-family GH16a enzymes (Figure 4; Michel *et al*., 2001). One key difference between the the XTHs and the (1,3-1,4)-β-D-glucanases is the insertion of three amino acid residues in the XTHs, at a position corresponding to $Pro_{118}Tyr_{119}Ile_{120}$ of the *Vigna angularis* XTH (Figure 3). An additional difference is the substitution of Met, at a position corresponding to Met180 of the *Bacillus macerans* (1,3;1,4)-β-D-glucanase (Figure 3b), with an aromatic amino acid residue, mostly Tyr, at a position corresponding to Tyr170 of the *Vigna angularis* XTH (Figures 3 and 6).

There are no 3D structures available for higher plant XTHs, although crystals that refract to less than 2 Å have been obtained for an XTH from *Populus tremula x tremuloides* (Johansson *et al.*, 2003). However, reliable models of the *Vigna angularis* XTH could be generated using solved 3D structures for (1,3;1,4)-β-D-glucanases from *Bacillus macerans* (Hahn *et al*., 1995; Figure 4; Table 1). Similarly, reliable models of the family GH16a non-specific (1,3/1,3;1,4)-β-D-glucanases could be generated using the known 3D structure of the *Pseudoalteromonas carragenovora* κ-carrageenase (Michel *et al*., 2001) as a template (Figure 4; Table 1), but reliable models could not be built from 3D structures across the sub-families GH16a and GH16b (Table 1). It must be remembered that generation of the models of XTHs necessitated the removal of 50-100 amino acid residues from their COOH-termini, and that this COOH-terminal region could play an important role in substrate specificity.

Thus, the homology modelling experiments established a 3D structural similarity between the XTHs and the (1,3;1,4)-β-D-glucanases of family GH16, and hence between proteins that bind xyloglucans and (1,3;1,4)-β-D-glucans. The substrate-binding cleft of the XTH appeared to be wider than that of the (1,3;1,4)-β-D-glucanase (Figure 4), and this might be related to the need for

XTHs to accommodate a (1,4)-β-D-glucan backbone that is substituted with relatively bulky xylosyl and other sugar moieties. In contrast to the apparent similarities between the XTHs and the (1,3;1,4)-β-D-glucanases of family GH16, structural links between the XTHs and (1,4)-β-D-xylan endohydrolases were not so obvious. There are no (1,4)-β-D-xylanases in family GH16; these enzymes are variously placed in families GH8, GH10 and GH11 (Coutinho and Henrissat, 1999). The protein folds detected for the glycosyl hydrolase families GH8, GH10 and GH11 that contain (1,4)-β-D-xylan endohydrolases are $(\alpha/\alpha)_6$, $(\beta/\alpha)_8$ and β-jelly roll, respectively (Coutinho and Henrissat, 1999). Because the family GH16 enzymes also adopt a β-jelly roll conformation and because the 3D structure of a family GH11 (1,4)-β-D-xylan endohydrolase from *Aspergillus niger* has been solved (Krengel and Dijkstra, 1996), it was possible to compare this structure with the model of the XTH from *Vigna angularis* (Figure 5). In addition, selected active site amino acid residues from the model prepared for the family GH16 XTH from *Vigna angularis* were shown to have a similar relative 3D disposition as those defined by the 3D structure of the family GH11 (1,4)-β-D-xylan endohydrolase from *Aspergillus niger* (Figure 6). These models therefore established a structural, and potential functional, linkage between the family GH16 XTHs and the family GH11 (1,4)-β-D-xylan endohydrolases.

Within the theoretical and practical constraints associated with homology modelling, and taking particular care to point out that some of the protein sequences were truncated before reliable models could be built, potential evolutionary and/or structural links have been established between family GH16 XTHs and (1,3;1,4)-β-D-glucanases, and between the XTHs and family GH11 (1,4)-β-D-xylan endohydrolases (Figures 4-6). In the context of seeking a potential role for the highly abundant XTHs of the Poaceae (Fry *et al.*, 1992; Wu *et al.*, 1994; Figure 1) in the hydrolysis or modification of polysaccharides other than the assumed substrate of xyloglucan, the homology modelling experiments suggest that the substrate-binding clefts and active sites of the XTHs are structurally similar to those of the (1,3;1,4)-β-D-glucanases and the (1,4)-β-D-xylan endohydrolases.

Thus, one can postulate that the XTHs of the Poaceae might have evolved to bind these other wall components. Higher plants already have (1,3;1,4)-β-D-glucanases and (1,4)-β-D-xylan endohydrolases from families other than GH16 and GH11, so one might further suggest that the need for XTHs with altered specificity in the Poaceae could be related to a requirement for the transglycosylation and attendant disproportionation of wall arabinoxylans and (1,3;1,4)-β-D-glucans, rather than a role in hydrolysis of these wall polysaccharides. The first evidence in support of this role was recently provided by Kerr and Fry (2003), who showed an abrupt increase in the molecular mass of xylans in walls of suspension-cultured maize cells in the first few hours after deposition in the walls. This is consistent with (1,4)-β-D-xylan transglycosylation activity, which could be catalysed by an XTH modified for action on (1,4)-β-D-xylans, and is reminiscent of the well-characterized action of XTHs on xyloglucans (Smith and Fry, 1991; Nishitani, 1997). Although it is likely to be difficult and time-consuming to separately purify the five XTH isoenzymes that correspond to the five most abundantly expressed XTH genes from barley (*HvXTH1* to *HvXTH5*; Figure 1), we have now cloned cDNAs for each of these barley genes (unpublished data) and will attempt to express active enzymes in heterologous systems, and to investigate whether any of the individual, expressed HvXTH enzymes, isolated in highly purified form, are active on arabinoxylans or (1,3;1,4)-β-D-glucans.

Experimental procedures

Database construction and evolutionary analyses

A total of about 250 amino acid sequences of family GH16 glycoside hydrolases was collected through an automated blast search from the NCBI-GenBank database (Benson *et al.*, 1999) using parsing tools from the LED (Fischer and Pleiss, 2003; http://www.ghdb.uni-stuttgart.de). Amino acid residues with potential roles in catalytic and substrate binding were annotated based on the information obtained by multiple sequence alignments with ClustalW (Thompson *et al.*, 1997). Phylogenetic trees were constructed with TREE-PUZZLE version 5.0 using maximum-likelihood and quartet-puzzling (Schmidt *et al.*, 2002). The parallel version of TREE-PUZZLE was run on a Linux PC-cluster of Dual Athlon MP 1800+ with eight processors and a Myrinet interconnect system. The phylogenetic trees were edited manually and were drawn with the TREE-PUZZLE program (Schmidt *et al.*, 2002). The accession numbers at the GenBank/EMBL, SWISS-PROT and Protein Data Bank (Berman *et al.,* 2000) databases of the 56 selected family GH16 glycoside hydrolases are as follows. The subgroup of "non-specific" (1,3/1,3;1,4)-β-D-glucan endohydrolases includes the entries from *Eisenia foetida* (O77072), *Bacillus circulans* (Q45095, P23903 and BAC06195), *Thermogota maritima* (B72428), *Thermotoga neapolitana* (Q60039), *Cochliobolus carbonum* (O14421), *Lysobacter enzymogenes* (AAN77505), *Oerskovia xanthineolytica* (O68641), *Strongylocentrotus purpuratus* (Q26660), *Streptomyces avermitilis MA-4680* (BAC69475), and the KRE6 protein from *Candida albicans* KRE6 (P87023). The subgroup of (1,4)-β-galactanases/κ-carrageenases includes the entries from *Zobellia galactanivorans* (O84907), *Pirellula sp.1* (CAD72787.1), *Pseudoalteromonas carrageenovora* (1DYP) and *Pirellula sp.* (CAD73010.1). The subgroup of (1,3)-β-galactanases includes the entries from uncultured bacterium AguB (AAP49346.1) and AguD (AAP49316.1), *Aeromonas sp.* (AAF03246), *Alteromonas atlantica* (Q59078), *Pseudomonas sp. Nd137* (BAB79291), *Zobellia galactanivorans* (AAF21820),

Microscilla sp. PRE1 (AAK62838), *Streptomyces coelicolor* (P07883) and *Streptomyces coelicolor* A3 (2) (NP_627674). The subgroup of (1,3;1,4)-β-D-glucanases includes entries from *Clostridium acetobutylicum* (D97245), *Clostridium thermocellum* (P29716), *Pseudomonas sp.* (BAC24104), *Orpinomyces sp. PC-2* (O14412), *Streptococcus bovis* (O07856), *Bacillus brevis* (P37073), *Brevibacillus brevis* (A48378), *Bacillus amyloliquefaciens* (P07980), *Bacillus subtilis* (P04957), *Bacillus lichiformis* (1GBG), *Hypocrea jecorina* (AAF82804), *Bacillus polymyxa* (P45797), *Bacillus macerans* (1BYH) and *Rhizobium meliloti* (P33693). Finally, the subgroup of XTH entries includes entries from *Carica papaya* (AAK51119), *Vitis labrusca* (BAB78506), *Arabidopsis thaliana* (AAM91637), *Daucus carota* (AAK30204), *Vigna angularis* (A49539), *Actinidia deliciosa* (AAC09388), *Hordeum vulgare* (X91659), *Nicotiana tabacum* (BAA13163), *Gossypium hirsutum* (T09870), *Cicer arietinum* (CAA06217), *Pisum sativum* (BAA34946), *Asparagus officialis* (AAF80591), *Beta vulgaris* (AAL04440), *Fagus sylvatica* (CAA10231), *Ananas comosus* (AAM28287.1), *Lycopersicon esculentum* (S49812) and *Festuca pratensis* (CAC40809).

Multiple sequence alignments

Multiple sequence alignments were performed with ClustalW 8.0 (Thompson *et al.* 1994; Higgins *et al.*, 1996; Thompson *et al.*, 1997; Jeanmougin *et al.*, 1998) using the LED database. Individual entries were checked manually by hydrophobic cluster analysis (Lemesle-Varloot *et al.*, 1990) to ensure that integrity of hydrophobic clusters was undisturbed and that both the distribution of secondary structure elements and topology of the active sites remained conserved. The program Bestfit from the University of Wisconsin GCG software package (Devereux *et al.*, 1984), with the implemented gap penalty function and the Smith and Waterman local algorithm (Smith and Waterman, 1981), was used to calculate sequence identities and similarities between the template and target protein sequences.

EST database analysis

Publicly available EST sequences from barley were accessed through the NCBi site (http://www.ncbi.nlm.nih.gov). A total of approximately 345,000 barley ESTs available in October 2003 was searched for sequences corresponding to enzymes and proteins involved in cell wall biosynthesis, modification and/or degradation. These included cellulose synthases (CesA), cellulose synthase-like enzymes (Csl), glucan synthase-like proteins (Gsl), α- and β-expansins, XTHs, β-D-glucan endo- and exohydrolases, (1,4)-β-D-xylan endo- and exohydrolases, (1,4)-β-D-mannan endohydrolases, and α-L-arabinofuranosidases. Stress-related (1,3)-β-D-glucan endohydrolases were specifically excluded from the analysis. No attempts were made to discriminate between isoforms of the various proteins or between individual EST libraries, and total numbers of ESTs were simply used as a first approximation of the relative abundance of mRNA transcripts in the range of tissues from which the EST libraries had been prepared. To estimate the number of genes in the barley *XTH* gene family, *XTH* sequences were aligned for the identification of overlapping EST sequences that corresponded to fragments of the same gene, and for the identification of distinct genes. ESTs with homology to previously identified barley and rice XTH genes were aligned and clustered using the ContigExpress program that is a part of the Vector NTi Suite 7.0 software package (Informax Inc., Maryland, MD, USA; http://www.informaxinc.com).

Homology protein structure modelling

The 3D molecular models of protein sequences of selected representatives of family GH16 glycoside hydrolases were constructed with Modeller 6v2, which is based on homology modelling by satisfaction of spatial restraints (Sali and Blundell, 1993). Default settings of the program Modeller 6v2 (Sali and Blundell, 1993) and the structurally optimised aligned protein sequences

were used. Homologous proteins exhibiting substrate specificities corresponding to non-specific (1,3/1,3;1,4)-β-D-glucanases, (1,3;1,4)-β-D-glucanases, (1,3)- and (1,4)-β-galactanases and XTHs were grouped. The NH_2-termini of the amino acid sequences were deduced from the literature data when available and/or in combination with multiple sequence alignments (Harvey *et al.*, 2000) and the PRODOM program that analyses domain arrangements (Gouzy *et al.*, 1996).

Evaluation of models

The stereochemical quality (Ramachandran plots) and overall G-factors of the final models, which are measures of normality of main chain bond lengths and bond angles (Engh and Huber 1991), were calculated with PROCHECK (Ramachandran *et al.,* 1963; Laskowski *et al.,* 1993). Further, the program "O" (Jones *et al.*, 1991) was applied for the calculation of root mean square (RMS) deviations between C^{α} positions of the template and target protein 3D structures. Newly derived 3D models were superposed with Swiss-PDBViewer V3.7 (Guex and Peitsch 1997) and viewed with PyMol (DeLano, 2002; http://www.pymol.org).

Acknowledgements

This work was supported by grants from the Federal Ministry of Education and Research, Germany (to J.P.) and from the Australian Research Council and the Grains Research and Development Corporation (to G.B.F.).

References

Anderson, M. A. and Stone, B. A. (1975) A new substrate for investigation the specificity of β-D-glucan hydrolases. *FEBS Lett* **52**, 202-207.

Bachman, E. S. and McClay, D. R. (1996) Molecular cloning of the first metazoan beta-1,3 glucanase from eggs of the sea urchin *Strongylocentrotus purpuratus*. *Proc Natl Acad Sci USA* **93**, 6808-6813.

Barbeyron, T., Gerard, A., Potin, P., Henrissat, B. and Kloareg, B. (1998) The kappa-carrageenase of the marine bacterium *Cytophaga drobachiensis*. Structural and phylogenetic relationships within family-16 glycoside hydrolases. *Mol Biol Evol* **15**, 528-7.

Benson, D. A., Boguski, M. S., Lipman, D. J., Ostell, J., Ouellette, B. F., Rapp, B. A. and Wheeler, D. L. (1999) GenBank. *Nucleic Acids Res* **27**, 12-17.

Berman, H. M., Westbrook, J., Feng, Z., Gilliland, G., Bhat, T. N., Weissig, H., Shindyalov, I. N. and Bourne, P. E. (2000) The Protein Data Bank. *Nucleic Acids Res* **28**, 235-242.

Carpita, N. C. and Gibeaut, D. M. (1993) Structural models of primary cell walls in flowering plants: consistency of molecular structure with the physical properties of the walls during growth. *Plant J* **3**, 1-30.

Carpita, N. C., Defernez, M., Findlay, K., Wells, B., Shoue, D. A., Catchpole, G., Wilson, R. H., McCann, M. C. (2001) Cell wall architecture of the elongating maize coleoptile. *Plant Physiol* **127,** 551-565.

Corpet, F., Gouzy, J. and Kahn, D. (1998) The ProDom database of protein domain families. *Nucleic Acids Res* **26**, 323-326.

Cosgrove, D. J. (1999) Enzymes and other agents that enhance cell wall extensibility. *Annu Rev Plant Physiol Plant Mol Biol* **50**, 391-417.

Coutinho, P. M. and Henrissat, B. (1999) Carbohydrate-active enzymes: an integrated database approach. In *Recent advances in carbohydrate bioengineering*, (Gilbert, H.J., Davies, G., Henrissat B. and Svensson B., eds.), The Royal Society of Chemistry, Cambridge, pp. 3-12. Carbohydrate-Active Enzymes server at http://afmb.cnrs-mrs.fr/~cazy/CAZY/index.html.

DeLano, W. L. (2002) The PyMOL Molecular Graphics System at URL: http://www.pymol.org.

Devereux, J., Haeberli, P. and Smithies, O. (1984) A comprehensive set of sequence analysis programs for the VAX. *Nucleic Acids Res* **12**, 387-395.

Engh, R. and Huber, R. (1991) Accurate bond and angle parameters for X-ray protein structure refinement. *Acta Crystallogr A* **47**, 392-400.

Farkas V., Sulova Z., Stratilova E., Hanna R. and Maclachlan, G. (1992) Cleavage of xyloglucan by nasturtium seed xyloglucanase and transglycosylation to xyloglucan subunit oligosaccharides. *Arch Biochem Biophys* **298**, 365-70.

Fanutti, C., Gidley, M. J. and Reid, J. S. G. (1993) Action of a pure xyloglucan endo-transglycosylase (formerly called xyloglucan-specific endo-(1-4)-β-D-glucanase) from the cotyledons of germinated nasturtium seeds. *Plant J* **3**, 691-700.

Fincher, G. B. (1993) Cell wall metabolism in barley. In *Barley: Genetics, Biochemistry, Molecular biology and Biotechnology*, (P. R. Shewry, ed.), CAB International, pp. 413-437.

Fischer, M. and Pleiss, J. (2003) The Lipase Engineering Database: a navigation and analysis tool for protein families. *Nucleic Acids Res* **31**, 319-321.

Fry, S. C. (1989) Cellulases, hemicellulases and auxin-stimulated growth: A possible relationship. *Physiol Plant* **72**: 532-536.

Fry S. C., Smith R. C., Renwick K. F., Martin D. J., Hodge S. K. and Matthews K. J. (1992) Xyloglucan endotransglycosylase, a new wall-loosening enzyme activity from plants. *Biochem J* **282**, 821-828.

Goff, S. A. (2002) Collaborating on the rice genome. *Science* **296**, 45-46.

Gouzy, J., Corpet, F. and Kahn, D. (1996) Graphical interface for ProDom domain families. *Trends Biochem Sci* **21**, 493.

Guex, N. and Peitsch, M. C. (1997) SWISS-MODEL and the Swiss-Pdb Viewer: An environment for comparative protein modeling. *Electrophoresis* **18**, 2714-2723.

Hahn, M., Keitel, T. and Heinemann, U. (1995) Crystal and molecular structure at 0.16-nm resolution of the hybrid *Bacillus* endo-1,3-1,4-beta-D-glucan 4-glucanohydrolase H(A16-M). *Eur J Biochem* **232**, 849-858.

Harvey, A. J., Hrmova, M., De Gori, R., Varghese, J. N. and Fincher, G. B. (2000) Comparative modeling of the three-dimensional structures of family 3 glycoside hydrolases. *Proteins* **41**, 257-269.

Hayashi, T. (1989) Xyloglucans in the primary cell wall. *Annu Rev Plant Physiol Plant Mol Biol* **40**, 139-168.

Higgins, D. G., Thompson, J. D. and Gibson, T. J. (1996) Using CLUSTAL for multiple sequence alignments. *Methods Enzymol* **266**, 383-402.

Høj, P. B. and Fincher, G. B. (1995) Molecular evolution of plant β-D-glucan endohydrolases. *Plant J* **7**, 367-379.

Hrmova, M. and Fincher, G. B. (2001) Structure-function relationships of β-D-glucan endo- and exohydrolases from higher plants. *Plant Mol Biol* **47**, 73-91.

Ishimaru, M. and Kobayashi, S. (2002) Expression of a xyloglucan endo-transglycosylase gene is closely related to grape berry softening. *Plant Sci* **162**, 621-628.

Jeanmougin, F., Thompson, J. D., Gouy, M., Higgins, D. G. and Gibson, T. J. (1998) Multiple sequence alignment with Clustal X. *Trends Biochem Sci* **23**, 403-405.

Johansson, P., Denman, S., Brumer, H., Kallas, A. M., Henriksson, H., Bergfors, T., Teeri, T. T., Jones, T. A. (2003) Crystallization and preliminary X-ray analysis of a xyloglucan endotransglycosylase from *Populus tremula x tremuloides*. *Acta Crystallogr D* **59**, 535-537.

Jones, T., Zou, J.-Y., Cowan, S. and Kjeldgaard, M. (1991) Improved methods for building protein models in electrone density maps and the location of errors in these models. *Acta Crystallogr A* **47**, 100-119.

Keitel, T., Simon, O., Borriss, R. and Heinemann, U. (1993) Molecular and active-site structure of a *Bacillus* 1,3-1,4-beta-glucanase. *Proc Natl Acad Sci USA* **90**, 5287-5291.

Kerr, E. M. and Fry, S. C. (2003) Pre-formed xyloglucans and xylans increase in molecular weight in three distinct compartments of a maize cell-suspension culture. *Planta* **217**, 327-339.

Kloareg, B. and Quatrano, R. S. (1988) Structure of the cell walls of marine algea and ecophysical functions of the matrix polysaccharides. *Oceanogr Mar Biol Annu Rev* **26**, 259-315.

Knogge, W. (2002) Avirulence determinants and elicitors. In *The Mycota, Vol. XI. Agricultural applications* (Kempken, F. ed.), Springer Verlag, Berlin, pp. 289-310.

Krengel, U. and Dijkstra, B. W. (1996) Three-dimensional structure of endo-1,4-beta-xylanase I from *Aspergillus niger*: molecular basis for its low pH optimum. *J Mol Biol* **263**, 70-78.

Laskowski, R. A., MacArthur, M. W., Moss, D. S. and Thornton, J. M. (1993) PROCHECK: a program to check the stereochemical quality of protein structures. *J Appl Cryst* **26**, 283-291.

Lemesle-Varloot, L., Henrissat, B., Gaboriaud, C., Bissery, V., Morgat, A. and Mornon, J. P. (1990) Hydrophobic cluster analysis: procedures to derive structural and functional information from 2-D-representation of protein sequences. *Biochimie* **72**, 555-574.

Louw, M. E., Reid, S. J. and Watson, T. G. (1993) Characterization, cloning and sequencing of a thermostable endo-(1,3-1,4)-beta-glucanase-encoding gene from an alkalophilic *Bacillus brevis*. *Appl Microbiol Biotechnol* **38**, 507-513.

Mengden, K., Hahn, M., Deisig, H. (1996) Morphogenesis and mechanisms of penetration by plant pathogenic fungi. *Annu Rev Phytopatol* **34**, 367-386.

Michel, G., Chantalat, L., Duee, E., Barbeyron, T., Henrissat, B., Kloareg, B. and Dideberg, O. (2001) The kappa-carrageenase of *P. carrageenovora* features a tunnel-shaped active site: a novel insight in the evolution of Clan-B glycoside hydrolases. *Structure* **9**, 513-525.

Nishitani, K. (1997) The role of endoxyloglucan transferase in the organization of plant cell wall. *Int Rev Cytol* **173**, 157-206.

Okazawa, K., Sato, Y., Nakagawa, T., Asada, K., Kato, I., Tomita, E. and Nishitani, K. (1993) Molecular cloning and cDNA sequencing of endoxyloglucan transferase, a novel class of glycosyltransferase that mediates molecular grafting between matrix polysaccharides in plant cell walls. *J Biol Chem* **268**, 25364-25368.

Pennel, R. (1998) Cell walls: structures and signals. *Curr Opin Plant Biol* **1**, 504-510.

Parrish, F. W., Perlin, A. S. and Reese, E.T . (1960) Selective enzymolysis of poly-β-D-glucans, and the structure of the polymers. *Can J Chem* **38**, 2094-2104.

Ramachandran, G. N., Ramakrishnan, C. and Sasisekharan, V. (1963) Stereochemistry of polypeptide chain configurations. *J Mol Biol* **7**, 95-99.

Rose, J. K. C., Braam, J., Fry, S. C. and Nishitani, K. (2002) The XTH family of enzymes involved in xyloglucan endotransglucosylation and endohydrolysis: Current perspectives and a new unifying nomenclature. *Plant Cell Physiol* **43**, 1421-1435.

Sali, A. and Blundell, T. L. (1993) Comparative protein modelling by satisfaction of spatial restraints. *J Mol Biol* **234**, 779-815.

Sakurai, N. and Masuda, Y. (1978) Auxin-induced changes in barley coleoptile cell wall composition. *Plant Cell Physiol* **19**, 1217-1223.

Schimming, S., Schwarz, W. H. and Staudenbauer, W. L. (1992) Structure of the *Clostridium thermocellum* gene licB and the encoded beta-1,3-1,4-glucanase. A catalytic region homologous to *Bacillus lichenase* joined to the reiterated domain of clostridial cellulases. *Eur J Biochem* **204**, 13-19.

Schmidt, H. A., Strimmer, K., Vingron, M. and von Haeseler, A. (2002) TREE-PUZZLE: maximum likelihood phylogenetic analysis using quartets and parallel computing. *Bioinformatics* **18**, 502-504.

Schünmann, P. H. D., Smith, R. C., Lang, V., Matthew, R.and Chandler, P. M. (1997)

Expression of XET-related genes and its relation to elongation in leaves of barley (*Hordeum vulgare* L.). *Plant Cell Env* **20**, 1439-1450.

Shibuya, N. and Misaki, A. (1978) Structure of hemicellulose isolated from rice endosperm cell wall: mode of linkages and sequences in xyloglucan, β-D-glucan and arabinoxylan. *Agric Biol Chem* **42**, 2267-2274.

Shibuya, N., Misaki, A. and Iwasaki, T. (1983) The structure of arabinoxylan and arabinoglucuronoxylan isolated from rice endosperm cell walls. *Agric Biol Chem* **47**, 2223-2230.

Smith, R. C. and Fry, S. C. (1991) Endotransglycosylation of xyloglucans in plant cell suspension cultures. *Biochem J* **279**, 529-535.

Smith, R. C., Matthews, P. R., Schünmann, P. H. D. and Chandler, P. M. (1997) The regulation of leaf elongation and xyloglucan endotransglycosylase by gibberellin in Himalaya barley (*Hordeum vulgare* L.) *J Exp Bot* **47**, 1395-1404.

Smith, T. F. and Waterman, M. S. (1981) Identification of common molecular subsequences. *J Mol Biol* **147**, 195-197.

Tahir, T. A., Berrin, J. G., Flatman, R., Roussel, A., Roepstorff, P., Williamson, G. and Juge, N. (2002) Specific characterization of substrate and inhibitor binding sites of a glycosyl hydrolase family 11 xylanase from *Aspergillus niger*. *J Biol Chem* **277**, 44035-44043.

Thompson, J. D., Gibson, T. J., Plewniak, F., Jeanmougin, F. and Higgins, D. G. (1997) The CLUSTAL_X windows interface: flexible strategies for multiple sequence alignment aided by quality analysis tools. *Nucleic Acids Res* **25**, 4876-4882.

Thompson, J. D., Higgins, D. G. and Gibson, T. J. (1994) CLUSTAL W: improving the sensitivity of progressive multiple sequence alignment through sequence weighting, position-specific gap penalties and weight matrix choice. *Nucleic Acids Res* **22**, 4673-4680.

Yahata, N., Watanabe, T., Nakamura, Y., Yamamoto, Y., Kamimiya, S. and Tanaka, H. (1990) Structure of the gene encoding beta-1,3-glucanase A1 of *Bacillus circulans* WL-12. *Gene* **86**, 113-117.

Wu Y., Spollen W. G., Sharp R. E., Hetherington P. R. and Fry S. C. (1994) Root growth maintenance at low water potentials (increased activity of xyloglucan endotransglycosylase and its possible regulation by abscisic acid). *Plant Physiol* **106**, 607-615.

Legends to Figures

Figure 1. Analysis of EST databases.

(A) Relative abundance of ESTs encoding cell wall modifying enzymes and proteins, taken from approximately 345,000 barley ESTs. Numbers indicate the actual number of EST entries for each class of enzyme or protein. CesA indicates cellulose synthase, Gsl indicates glucan synthase-like proteins, Ara/Xyl indicates α-L-arabinofuranosidases and β-D-xylosidases, and AXAH indicates arabinoxylan arabinofuranohydrolases.

(B) Relative abundance of ESTs encoding XTHs in the barley EST databases. The five most abundantly represented genes are designated *HvXTH1* (equivalent to *PM2*, Smith *et al*., 1997), *HvXTH2* (equivalent to *PM5*, Schünmann *et al*., 1997), *HvXTH3* (equivalent to *XEA*, Schünmann *et al*., 1997), *HvXTH4* (equivalent to *XEB*, Schünmann *et al.*, 1997), and *HvXTH5* (equivalent to *EXT*, Smith *et al*., 1997). The un-named relatively low abundance ESTs are likely to arise from nine separate genes.

Figure 2. Phylogenetic analysis of genes encoding family GH16 glycosyl hydrolases.

The phylogenetic tree is constructed from a selection of 56 members of family GH16 glycosyl hydrolases (Courtinho and Henrissat, 1999). Species names and descriptions of catalytic functions together with GenBank/EMBL, SWISS-PROT or PDB accession numbers are given for each enzyme. The enzymes can be divided into five groups, which fall within the two subfamilies GH16a and GH16b. Subfamily GH16a includes "non-specific" (1,3/1,3;1,4)-β-D-glucan endohydrolases (boxed in blue), (1,3)-β-galactanases (boxed in green) and (1,4)-β-galactanases/κ-carrageenases (boxed in deep blue). Subfamily GH16b includes (1,3;1,4)-β-D-

glucan endohydrolases (boxed in orange) and higher plant XTHs (boxed in red). The available 3D structures are shaded in red and the modelled 3D protein structures are coloured in blue. The phylogenetic trees were generated with TreePuzzle (Schmidt *et al*., 2002).

Figure 3. Multiple sequence alignments of the modelled (target) sequences and the 3D structures used as templates.

The enzymes of family GH16 are divided into the two subfamilies GH16a (panel A) and 16b (panel B). The numbers above the sequences in panels A and B indicate amino acid residues of 3D structures of the (1,4)-β-galactanase/κ-carrageenase from *Pseudoalteromonas carragenovorans* (Michel *et al*., 2001) and of the (1,3;1,4)-β-D-glucan endohydrolase from *Bacillus macerans* (Hahn *et al.,* 1995), respectively. Multiple sequence alignments of amino acid residues in the indicated regions show the difference between subfamily GH16a enzymes, comprising the (1,4)-β-galactanases/κ-carrageenases and the "non-specific" (1,3/1,3;1,4)-β-D-glucanase subgroups. Subfamily GH16b contains the XTHs and the (1,3;1,4)-β-D-glucanases. In subfamily GH16a four amino acid residues separate the catalytic Glu residues (coloured in red), while in subfamily GH16b three amino acid residues separate the catalytic Glu residues. Conserved hydrophobic residues (yellow), residues potentially involved in catalytic amino acid function (blue), and the conserved aromatic platform amino acid residues (green) are also indicated. The positions of these amino acid residues in the 3D structures and molecular models are shown in Figures 4-6. Putative Ca^{2+}-binding amino acid residues (aqua blue) and non-aromatic substrate binding residues (orange) are also shown. The PYX motif that is

inserted in the XTHs is shaded in gray/yellow in panel B. The multiple sequence alignments were calculated using ClustalW (Thompson *et al*., 1994).

Figure 4. Molecular surface representations of family GH16 enzymes.

Family GH16a members include the 3D structure of the *Pseudoalteromonas carragenovora* (1,4)-β-galactanase/κ-carrageenase (panel A), and the model of the *Strongylocentrotus purpuratus* "non-specific" (1,3/1,3;1,4)-β-D-glucanase (panel B). The family GH16b members are shown as the 3D structure of the *Bacillus macerans* (1,3;1,4)-β-D-glucanase (panel C), and the model of the *Vigna angularis* XTH (panel D). The catalytic amino acid residues are coloured in red, amino acid residues affecting the function of catalytic amino acid residues are blue, aromatic amino acid residues are in yellow and the distinguishing aromatic platform residues (Tyr, Trp or Phe) are highlighted in green. The Figure was generated using the PyMol program (DeLano *et al*., 2002).

Figure 5. Comparison of molecular surface representations of family GH11 and GH16 enzymes.

The 3D structure of a family GH11 (1,4)-β-D-xylan endohydrolase from *Aspergillus niger* is shown in panel A, and a model of the family GH16 XTH from *Vigna angularis* in panel B. The similarities in disposition of the catalytic (red) and the aromatic (yellow) amino acid residues at the bottom of the substrate binding clefts are shown. The Figure was generated using the PyMol program (DeLano *et al*., 2002).

Figure 6. Comparison of the 3D dispositions of amino acid residues in the active site regions of enzymes from families GH16 and GH11.

Active site amino acid residues from the 3D structure of the family GH16 (1,3;1,4)-β-D-glucanase from *Bacillus macerans* (panel A) are compared with those from the family GH16 XTH model from *Vigna angularis* (panel B), and with those from the 3D structure of the family GH11 (1,4)-β-D-xylan endohydrolase from *Aspergillus niger* (panel C). The catalytic amino acid residues are shown in red and the Asp residue between the two catalytic residues (Figure 3) is shown in cyan. The distinguishing aromatic amino acid residues are coloured in green and the aromatic residues that might be involved in substrate binding are coloured in yellow. In all but the two catalytic residues, the nitrogen and oxygen atoms are coloured in blue and red, respectively. Red circles show the conserved "aromatic triad". The Figure was generated using the PyMol program (DeLano *et al*., 2002).

Table 1 Evaluation of molecular models generated for selected enzymes from family GH16 glycosyl hydrolases.

Entry[a]	Activity[b]	Identity[c] %	RMS[d] Å (aa)	G-factor[e]	Ramachandran values[f] %	
					Allowed	Disallowed
Templates[g]						
1. *Bacillus macerans*	(1,3;1,4)	100	- (214)	-0.75	100	0
2. *Bacillus licheniformis*	(1,3;1,4)	100	- (214)	0.16	99.5	0.5
3. *Pseudoalteromonas carragenovora*	(κ-carrag)	100	- (271)	0.26	100	0
Targets[g]						
1. *Clostridium thermocellum*	(1,3;1,4)	59	0.4 (211)	-0.16	99.4	0.6
1. *Bacillus brevis*	(1,3;1,4)	58	0.4 (211)	-0.18	100	0
1. *Vitis labrusca*	(XET)	28	1.1 (171)	-0.46	97.6	2.4
2. *Vigna angularis*	(XET)	30	1.3 (163)	-0.50	98	2
3. *Zobellia galactanivorans*	(κ-carrag)	40	0.4 (244)	-0.29	98.7	1.3
3. *Bacillus circulans*	(1,3/1,3;1,4)	32	0.7 (202)	-0.44	98.7	0.3
3. *Strongylocentrotus purpuratus*	(1,3/1,3;1,4)	22	1.1 (256)	-0.50	99.1	0.9

[a] Representatives were chosen from different branches on the unrooted phylogenetic radial tree.

[b] Indicates enzymatic activity of the entry.

[c] Using Bestfit program of the University of Wisconsin GCG package (Devereux *et al.,* 1984).

[d] RMS deviations of the C^{α} backbone were determined using program "O" (Jones *et al.,* 1991). Numbers in brackets indicate the number of amino acid residues aligned to calculate the RMS deviations.

[e] Overall G-factors of models were calculated by PROCHECK (Laskowski *et al.,* 1993).

[f] Ramachandran plot statistics excluding Gly and Pro residues.

[g] The templates for *Clostridium, Bacillus brevis,* and *Vitis* was *Bacillus macerans* enzyme (Keitel *et al.*, 1993; 1BYH); for *Vigna* was *Bacillus licheniformis* enzyme (Hahn *et al.*, 1995; 1GBG); for *Zobellia*, *Bacillus circulans* and *Strongylocentrotus* was *Pseudoalteromonas* enzyme (Michel *et al.*, 2001; 1DYP).

Table 2 Frequencies of conservation of selected amino acid residues in family GH16 XTHs and (1,3;1,4)-β-D-glucanases. Amino acid residues having the same position are aligned with each other in the Table.

XTHs						
Residue[a]	Tyr75[d]	His83	Tyr99[d]	Phe106	Tyr170[d]	Trp174[d]
Frequency[b]	96	75(90)	77(92)	49(100)	76(84)	96
(1,3;1,4)-β-D-Glucanases						
Residue[a]	Phe92	Trp103	-	Tyr123	Met180	Trp184
Frequency[b]	96	75(90)	77(92)	49(100)	79	96

[a] Amino acid residues in XTHs corresponding to residues of the *Vigna angularis* enzyme.

[b] Frequencies are expressed in %. The numbers in parentheses are the frequencies of all aromatic amino acid residues observed in that position.

[c] Amino acid residues in (1,3;1,4)-β-D-glucanases corresponding to residues of the *Bacillus macerans* enzyme.

[d] These residues have the same 3D position in the XTHs and in the β-D-xylan endohydrolases, and are designated the "aromatic triad".

(a)

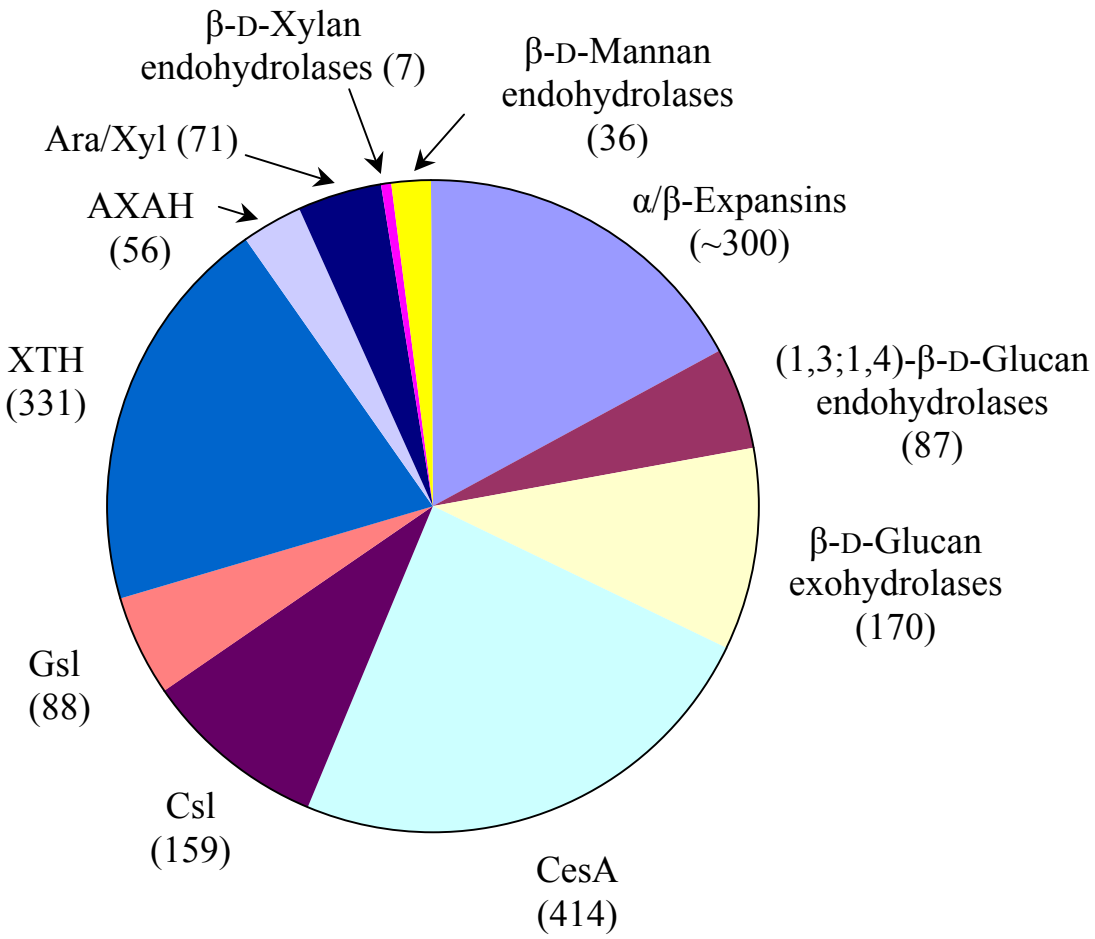
β-D-Xylan endohydrolases (7)
β-D-Mannan endohydrolases (36)
Ara/Xyl (71)
AXAH (56)
α/β-Expansins (~300)
XTH (331)
(1,3;1,4)-β-D-Glucan endohydrolases (87)
β-D-Glucan exohydrolases (170)
Gsl (88)
Csl (159)
CesA (414)

(b)

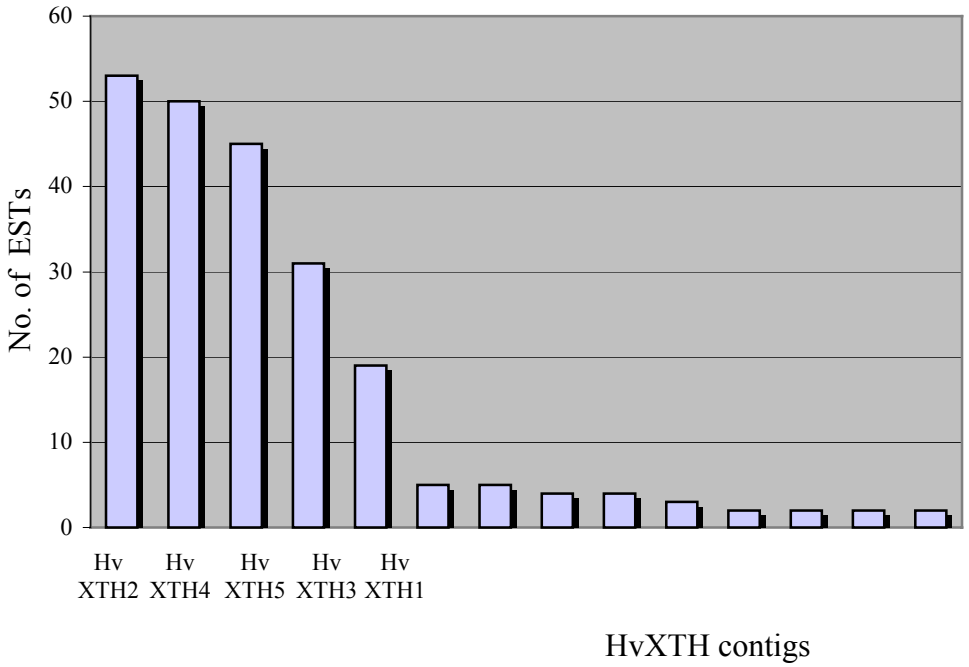
60
50
40
30
20
10
0
No. of ESTs
Hv XTH2
Hv XTH4
Hv XTH5
Hv XTH3
Hv XTH1
HvXTH contigs

Figure 1

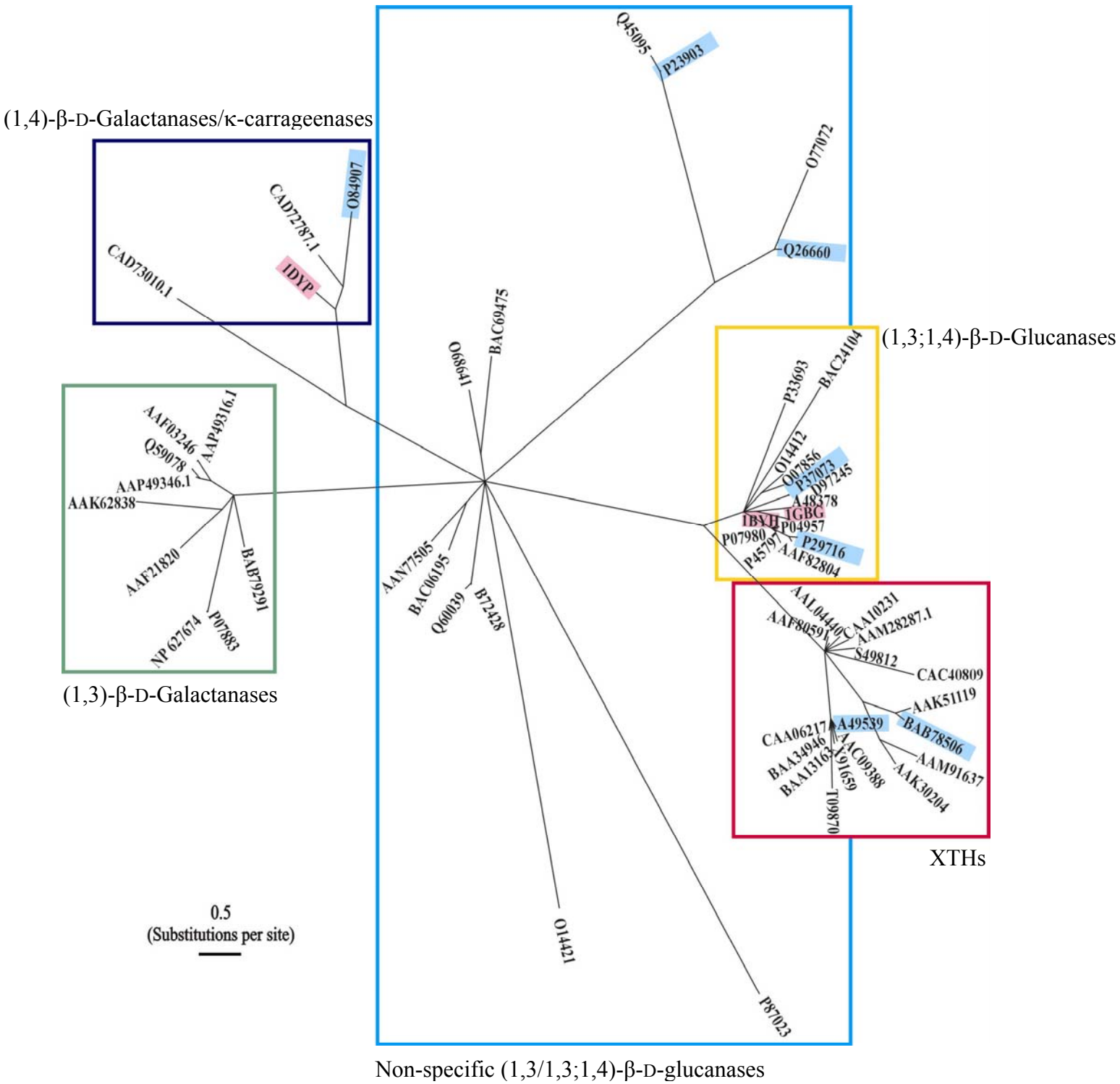
(1,4)-β-D-Galactanases/κ-carrageenases
CAD72787.1
Q84907
CAD73010.1
IDYP
(1,3)-β-D-Galactanases
AAF03246
AAP49316.1
Q59078
AAP49346.1
AAK62838
AAF21820
BAB79291
NP 627674
P07883
Q45095
P23903
O77072
Q26660
O68641
BAC69475
(1,3;1,4)-β-D-Glucanases
P33693
BAC24104
O14412
O07856
P37073
D97245
A48378
IGBG
IBYH
P04957
P07980
P45797
P29716
AAF82804
AAN77505
BAC06195
Q60039
B72428
AAL04440
AAF80591
CAA10231
AAM28287.1
S49812
CAC40809
AAK51119
CAA06217
A49539
BAB78506
BAA34946
BAA13163
AAC09388
AAM91637
T09870
AAK30204
XTHs
0.5
(Substitutions per site)
O14421
P87023
Non-specific (1,3/1,3;1,4)-β-D-glucanases

Figure 2

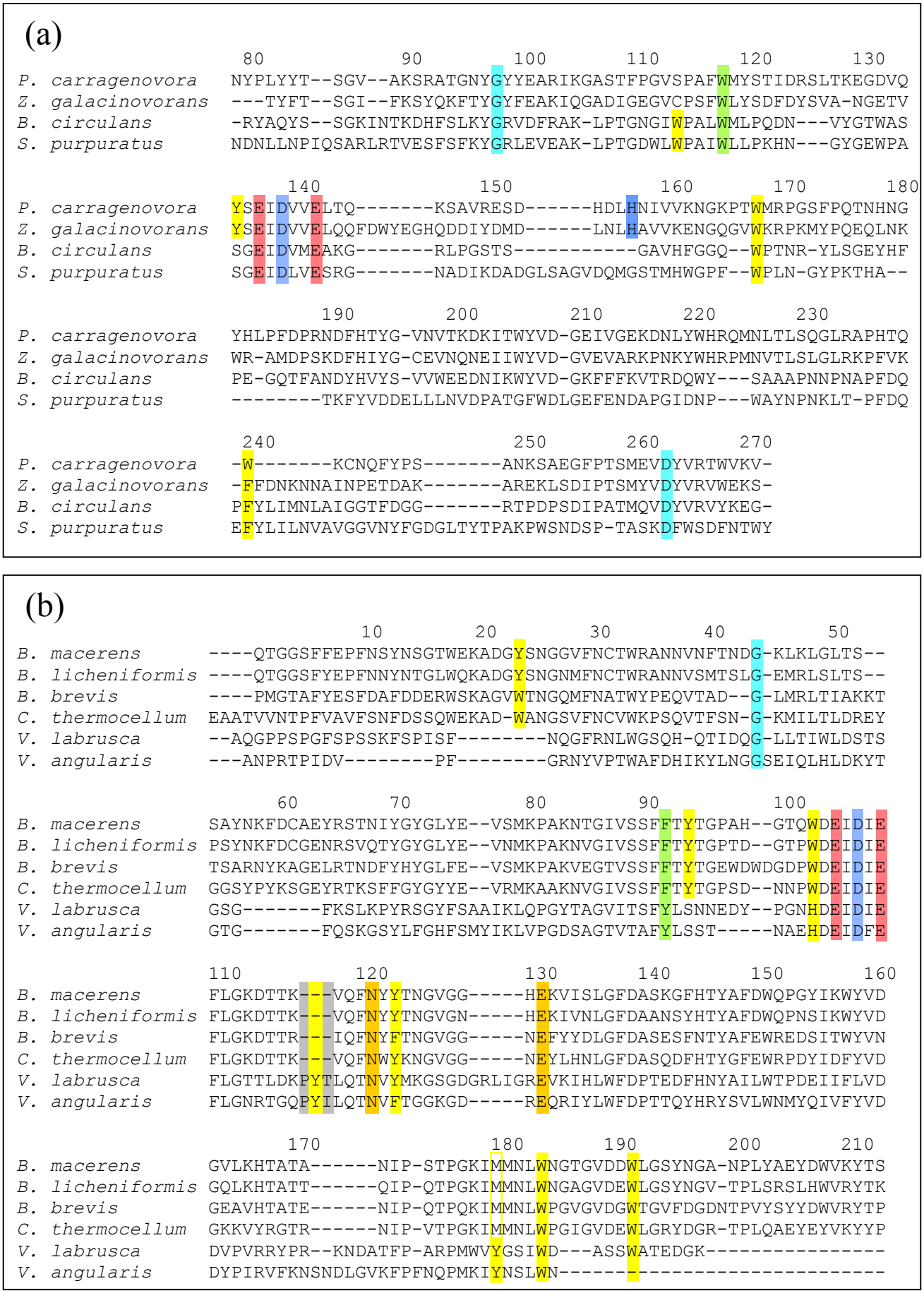
(a)
80 90 100 110 120 130
P. carragenovora NYPLYYT--SGV--AKSRATGNYGYYEARIKGASTFPGVSPAFWMYSTIDRSLTKEGDVQ
Z. galacinovorans ---TYFT--SGI--FKSYQKFTYGYFEAKIQGADIGEGVCPSFWLYSDFDYSVA-NGETV
B. circulans -RYAQYS--SGKINTKDHFSLKYGRVDFRAK-LPTGNGIWPALWMLPQDN---VYGTWAS
S. purpuratus NDNLLNPIQSARLRTVESFSFKYGRLEVEAK-LPTGDWLWPAIWLLPKHN---GYGEWPA
140 150 160 170 180
P. carragenovora YSEIDVVELTQ-------KSAVRESD------HDLHNIVVKNGKPTWMRPGSFPQTNHNG
Z. galacinovorans YSEIDVVELQQFDWYEGHQDDIYDMD------LNLHAVVKENGQGVWKRPKMYPQEQLNK
B. circulans SGEIDVMEAKG-------RLPGSTS-----------GAVHFGGQ--WPTNR-YLSGEYHF
S. purpuratus SGEIDLVESRG-------NADIKDADGLSAGVDQMGSTMHWGPF--WPLN-GYPKTHA--
190 200 210 220 230
P. carragenovora YHLPFDPRNDFHTYG-VNVTKDKITWYVD-GEIVGEKDNLYWHRQMNLTLSQGLRAPHTQ
Z. galacinovorans WR-AMDPSKDFHIYG-CEVNQNEIIWYVD-GVEVARKPNKYWHRPMNVTLSLGLRKPFVK
B. circulans PE-GQTFANDYHVYS-VVWEEDNIKWYVD-GKFFFKVTRDQWY---SAAAPNNPNAPFDQ
S. purpuratus --------TKFYVDDELLLNVDPATGFWDLGEFENDAPGIDNP---WAYNPNKLT-PFDQ
240 250 260 270
P. carragenovora -W-------KCNQFYPS-------ANKSAEGFPTSMEVDYVRTWVKV-
Z. galacinovorans -FFDNKNNAINPETDAK-------AREKLSDIPTSMYVDYVRVWEKS-
B. circulans PFYLIMNLAIGGTFDGG-------RTPDPSDIPATMQVDYVRVYKEG-
S. purpuratus EFYLILNVAVGGVNYFGDGLTYTPAKPWSNDSP-TASKDFWSDFNTWY
(b)
10 20 30 40 50
B. macerens ----QTGGSFFEPFNSYNSGTWEKADGYSNGGVFNCTWRANNVNFTNDG-KLKLGLTS--
B. licheniformis ----QTGGSFYEPFNNYNTGLWQKADGYSNGNMFNCTWRANNVSMTSLG-EMRLSLTS--
B. brevis ----PMGTAFYESFDAFDDERWSKAGVWTNGQMFNATWYPEQVTAD--G-LMRLTIAKKT
C. thermocellum EAATVVNTPFVAVFSNFDSSQWEKAD-WANGSVFNCVWKPSQVTFSN-G-KMILTLDREY
V. labrusca --AQGPPSPGFSPSSKFSPISF--------NQGFRNLWGSQH-QTIDQG-LLTIWLDSTS
V. angularis ---ANPRTPIDV--------PF--------GRNYVPTWAFDHIKYLNGGSEIQLHLDKYT
60 70 80 90 100
B. macerens SAYNKFDCAEYRSTNIYGYGLYE--VSMKPAKNTGIVSSFFTYTGPAH--GTQWDEIDIE
B. licheniformis PSYNKFDCGENRSVQTYGYGLYE--VNMKPAKNVGIVSSFFTYTGPTD--GTPWDEIDIE
B. brevis TSARNYKAGELRTNDFYHYGLFE--VSMKPAKVEGTVSSFFTYTGEWDWDGDPWDEIDIE
C. thermocellum GGSYPYKSGEYRTKSFFGYGYYE--VRMKAAKNVGIVSSFFTYTGPSD--NNPWDEIDIE
V. labrusca GSG-------FKSLKPYRSGYFSAAIKLQPGYTAGVITSFYLSNNEDY--PGNHDEIDIE
V. angularis GTG-------FQSKGSYLFGHFSMYIKLVPGDSAGTVTAFYLSST-----NAEHDEIDFE
110 120 130 140 150 160
B. macerens FLGKDTTK---VQFNYYTNGVGG-----HEKVISLGFDASKGFHTYAFDWQPGYIKWYVD
B. licheniformis FLGKDTTK---VQFNYYTNGVGN-----HEKIVNLGFDAANSYHTYAFDWQPNSIKWYVD
B. brevis FLGKDTTR---IQFNYFTNGVGG-----NEFYYDLGFDASESFNTYAFEWREDSITWYVN
C. thermocellum FLGKDTTK---VQFNWYKNGVGG-----NEYLHNLGFDASQDFHTYGFEWRPDYIDFYVD
V. labrusca FLGTTLDKPYTLQTNVYMKGSGDGRLIGREVKIHLWFDPTEDFHNYAILWTPDEIIFLVD
V. angularis FLGNRTGQPYILQTNVFTGGKGD-----REQRIYLWFDPTTQYHRYSVLWNMYQIVFYVD
170 180 190 200 210
B. macerens GVLKHTATA------NIP-STPGKIMMNLWNGTGVDDWLGSYNGA-NPLYAEYDWVKYTS
B. licheniformis GQLKHTATT------QIP-QTPGKIMMNLWNGAGVDEWLGSYNGV-TPLSRSLHWVRYTK
B. brevis GEAVHTATE------NIP-QTPQKIMMNLWPGVGVDGWTGVFDGDNTPVYSYYDWVRYTP
C. thermocellum GKKVYRGTR------NIP-VTPGKIMMNLWPGIGVDEWLGRYDGR-TPLQAEYEYVKYYP
V. labrusca DVPVRRYPR--KNDATFP-ARPMWVYGSIWD---ASSWATEDGK----------
V. angularis DYPIRVFKNSNDLGVKFPFNQPMKIYNSLWN-------

Figure 3

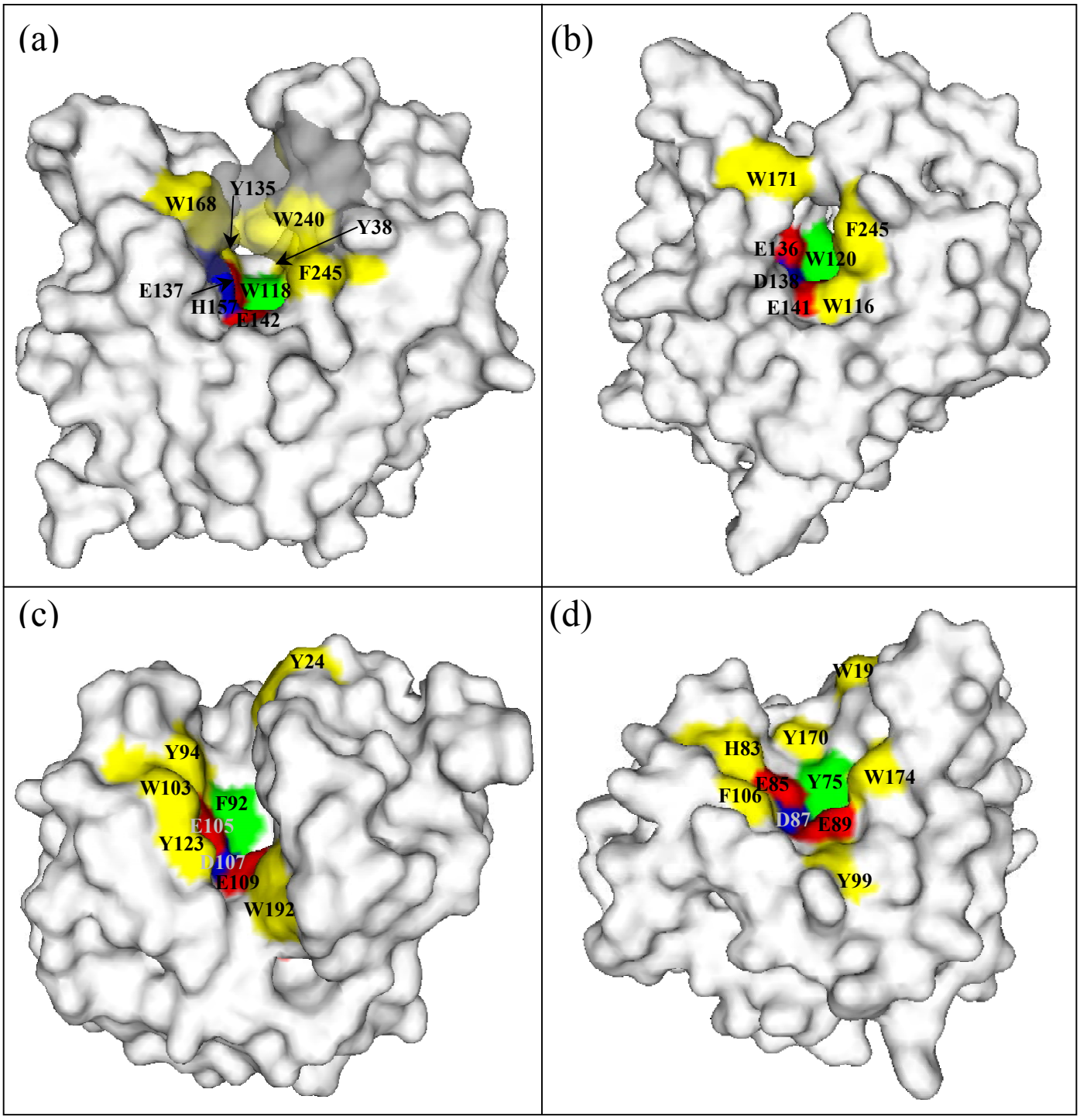
(a)
Y135
W168
W240
Y38
F245
E137
W118
H157
E142
(b)
W171
F245
E136
W120
D138
E141
W116
(c)
Y24
Y94
W103
F92
E105
Y123
D107
E109
W192
(d)
W19
H83
Y170
E85
Y75
W174
F106
D87
E89
Y99

Figure 4

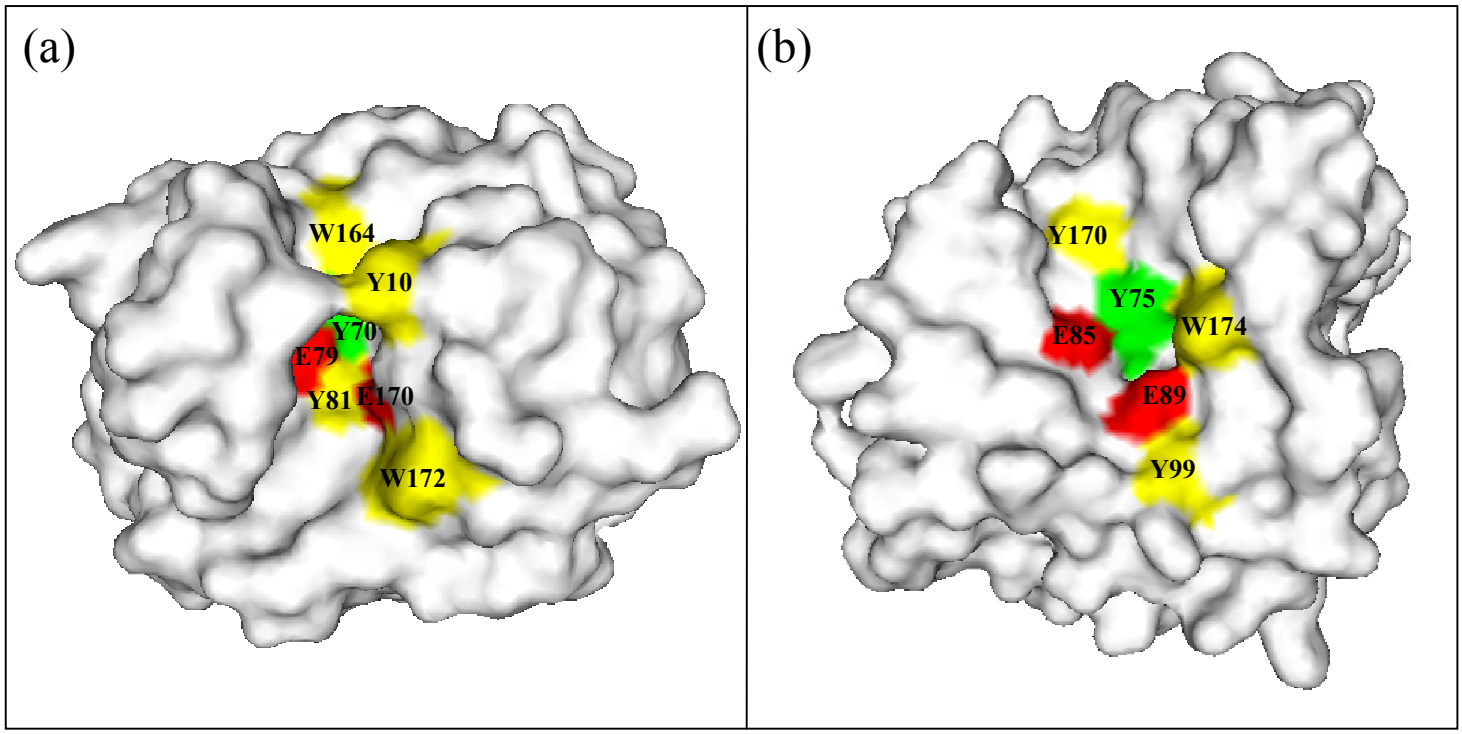

Figure 5

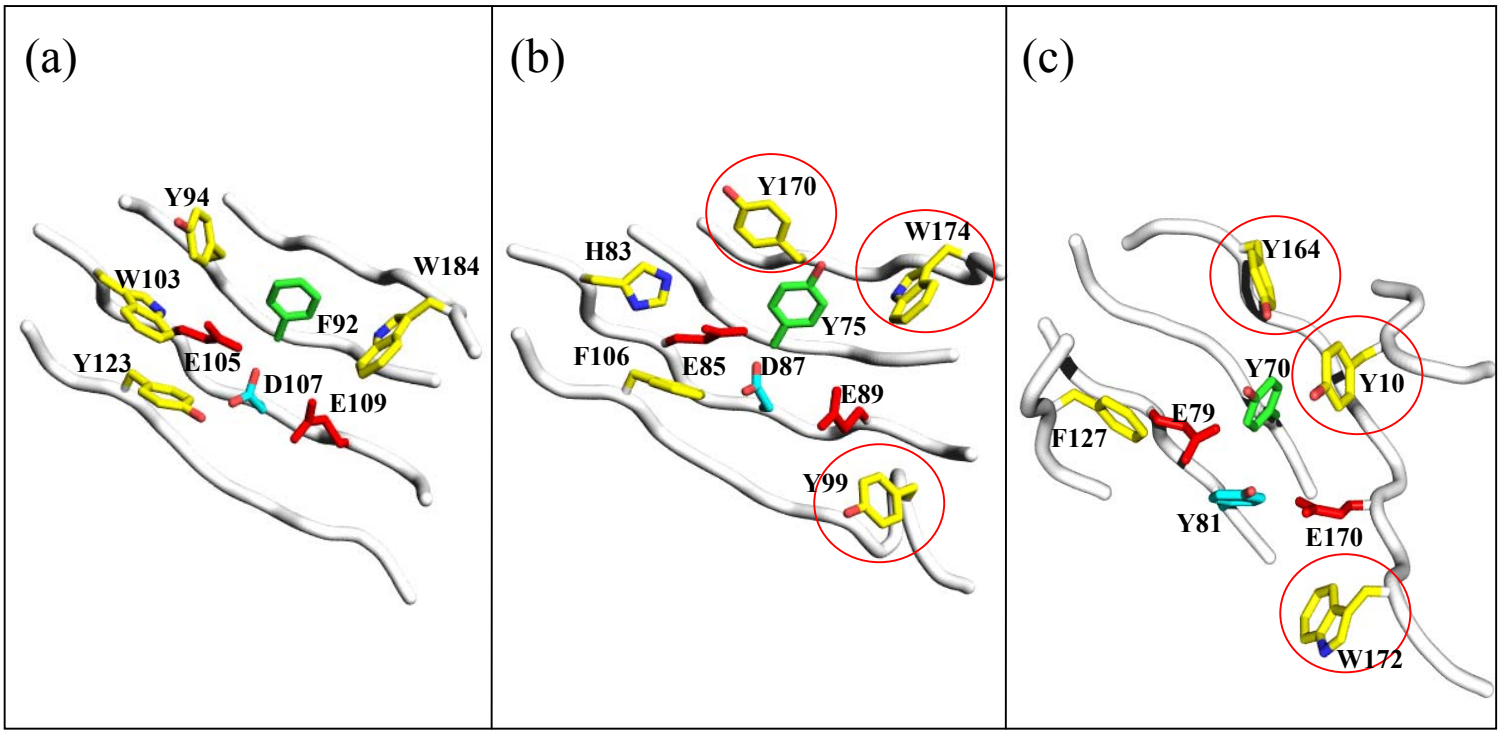
(a)
Y94
W184
W103
F92
Y123
E105
D107
E109
(b)
Y170
W174
H83
Y75
F106
E85
D87
E89
Y99
(c)
Y164
Y70
Y10
E79
F127
Y81
E170
W172

Figure 6